

iScience, Volume 25

Supplemental information

Experimental evolution of *Bacillus subtilis* on *Arabidopsis thaliana* roots reveals fast adaptation and improved root colonization

Mathilde Nordgaard, Christopher Blake, Gergely Maróti, Guohai Hu, Yue Wang, Mikael Lenz Strube, and Ákos T. Kovács

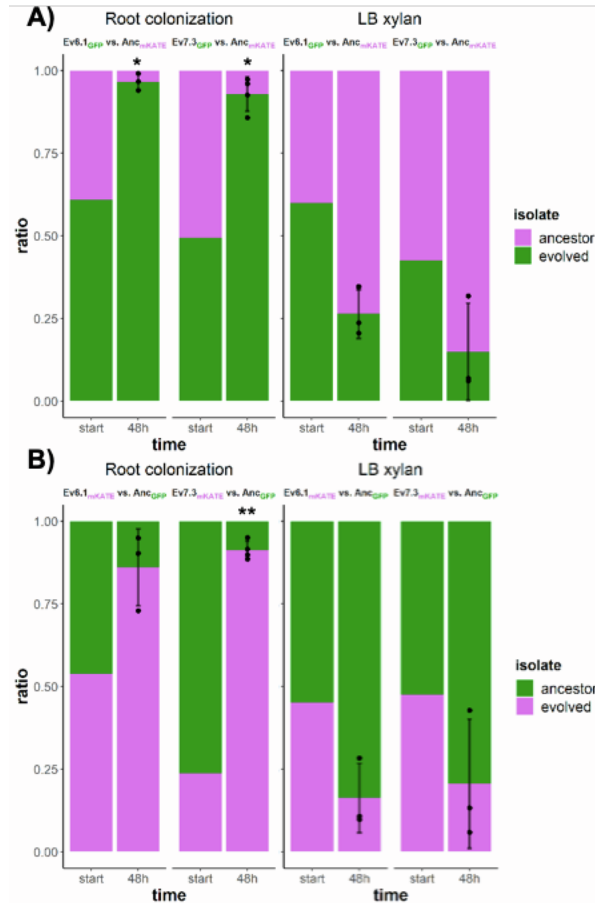


Figure S1: Competition between selected evolved isolates and the ancestor during root colonization and in LB xylan under shaking conditions. Related to Figure 4. **(A)** Competition between ancestor (magenta) and evolved isolates (green) during root colonization (left) and in LB xylan (0.5 %) under shaking conditions (right) for 48 h. **(B)** Same as in A, but with opposite fluorescent labels. The bar plots show the starting ratio of the evolved isolate and ancestor in the mix, and the observed ratios after 48 hours. Bars represent the mean (N=3-4) and the error bars represent standard deviation. The points show the replicates for the evolved (from below) and ancestor (from above). For statistical analysis, the relative fitness (r) of the evolved isolates was calculated by comparing the frequency of the evolved isolate at the beginning and at the end of the competition experiment. The \log_2 -transformed relative fitness values were subjected to a One-sample t -test to test whether the mean was significantly different from 0. * and ** indicate $P < 0.05$ and $P < 0.01$, respectively.

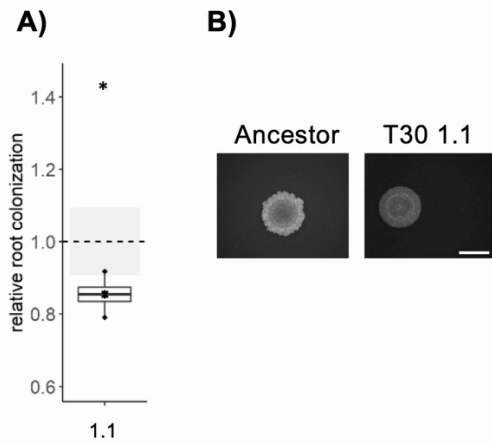


Figure S2: Relative root colonization and colony morphology of an evolved isolate from population 1 at the final transfer. Related to Figure 3. **(A)** Isolate Ev1.1 from transfer 30 was tested for individual root colonization. Relative root colonization was calculated by dividing the log₁₀-transformed productivity (CFU/mm root) of each replicate by the mean of the log₁₀-transformed productivity of the ancestor. The cross represents the mean relative root colonization (N=4). The dashed, horizontal line represents the mean of the ancestor (N=4), while the grey-shaded rectangles represent the standard deviation of the ancestor. The normalized values were subjected to a One-sample *t*-test to test whether the mean was significantly different from 1. * indicates $P < 0.05$. **(B)** ON cultures of the ancestor and Ev1.1 were spotted on LB agar (1.5 %) and imaged after incubation for 48 h at 30 °C using the stereomicroscope. Ancestor represents *B. subtilis* DK1042. Each colony is representative of at least three replicates. Scale bar denotes 5 mm.

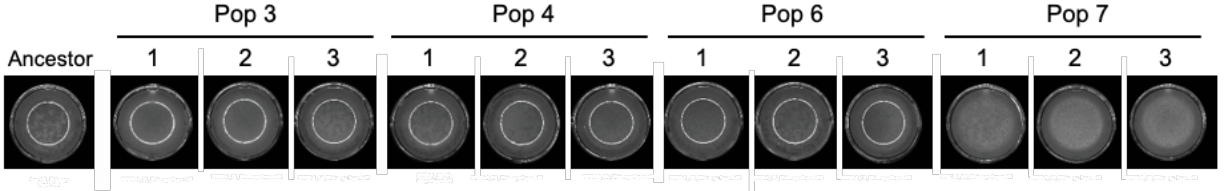


Figure S3: Pellicle biofilm formation in LB of the ancestor and evolved isolates from the final transfer. Related to Figure 5. *B. subtilis* ancestor and evolved isolates from transfer 30 were inoculated into LB medium at a starting OD₆₀₀ of 0.05 in 24-well plates and incubated for 48 h at 30 °C. Each image is representative of 3-4 replicates. The wells are 16 mm width.

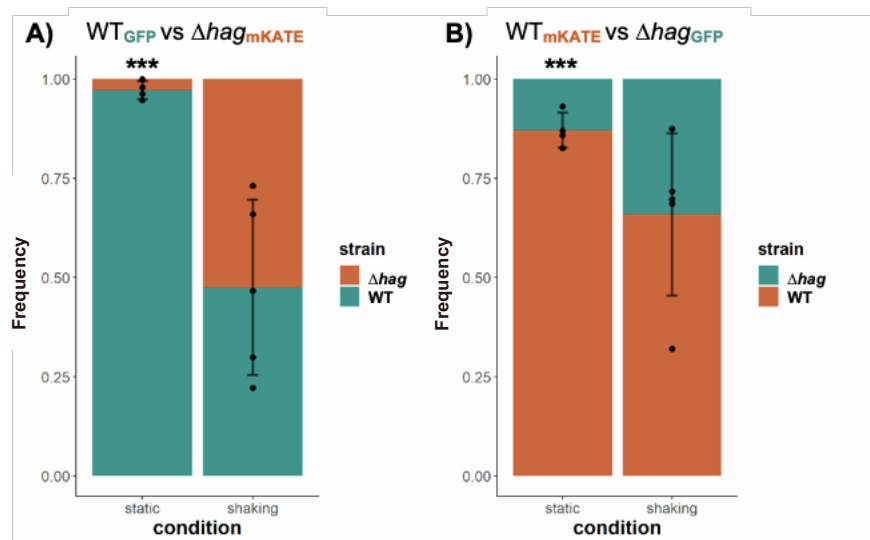


Figure S4: Motility is not important for root colonization under shaking conditions. Related to Figure 5. Competition between *B. subtilis* DK1042 (WT) and a Δhag mutant during root colonization in MSNg medium. *A. thaliana* seedlings were inoculated with a 1:1 mix of WT and mutant with opposite fluorescent labels at a starting $OD_{600}=0.02$. Plates were incubated for 48 h in the plant chamber under static conditions or shaking conditions (200 rpm). After three successive rounds of root colonization, productivity on the third root was quantified as CFU per cm root. **(A)** Competition between WT (turquoise) and the Δhag mutant (orange). **(B)** Same as in A, but with opposite fluorescent labels. Bars represent the mean ratio (N=4-5) and the error bars represent standard deviation. The points show the replicates for the WT (from below) and the Δhag mutant (from above). The observed frequencies of the WT after 48 h (on the third root) were divided by 0.5 (the starting frequency in the inoculation mix), and the resulting normalized values were subjected to a One-sample *t*-test to test whether the mean was significantly different from 1. *** indicates $P<0.001$.

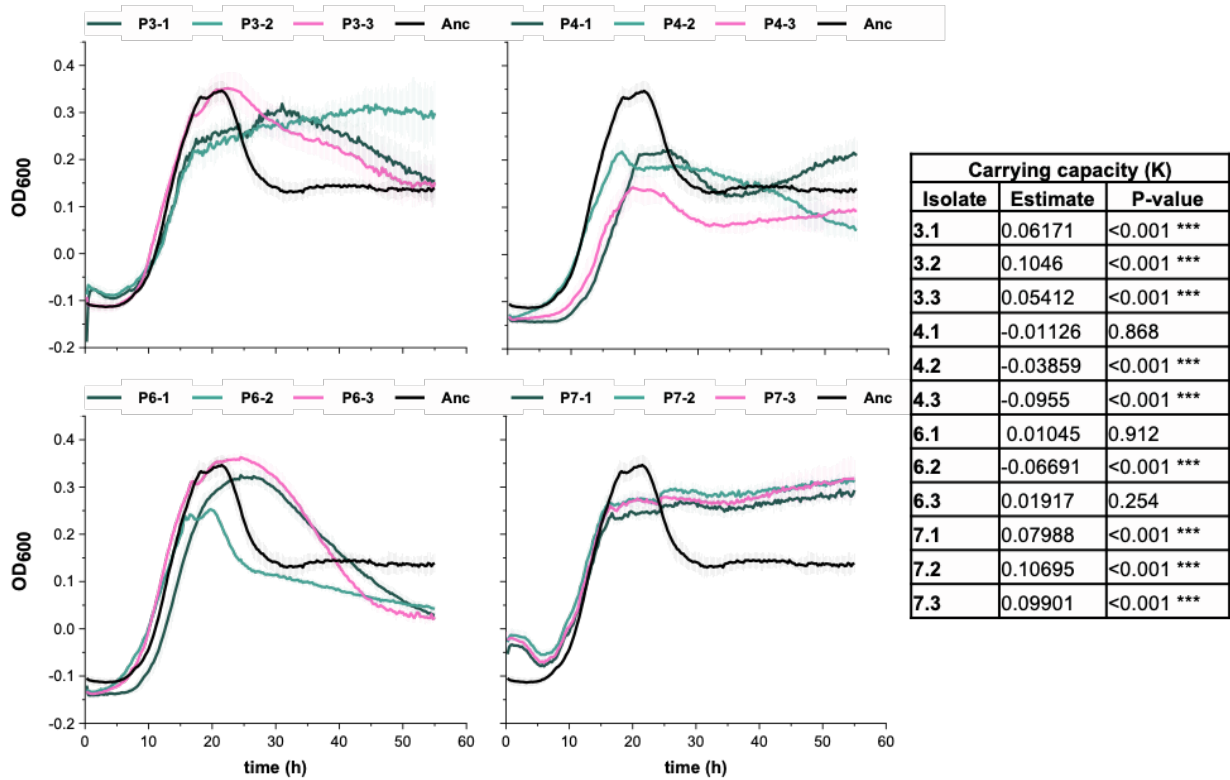


Figure S5: Growth of *B. subtilis* ancestor and evolved isolates in MSNc + xylan. Related to Figure 5. Growth of the ancestor and evolved isolates in MSNc + xylan (0.5 %) (starting $OD_{600} = 0.1$) was measured every 15 min at 24 °C under shaking conditions (orbital). Data represents mean and error bars represent standard deviation (N=6-12, 2 independent ON cultures with 3-6 technical replicates each). The carrying capacity (K) was calculated using “Growthcurver” in R. Significant difference between ancestor and evolved isolates was tested by an ANOVA followed by a Dunnett’s Multiple Comparison test. *** indicates $P < 0.001$.

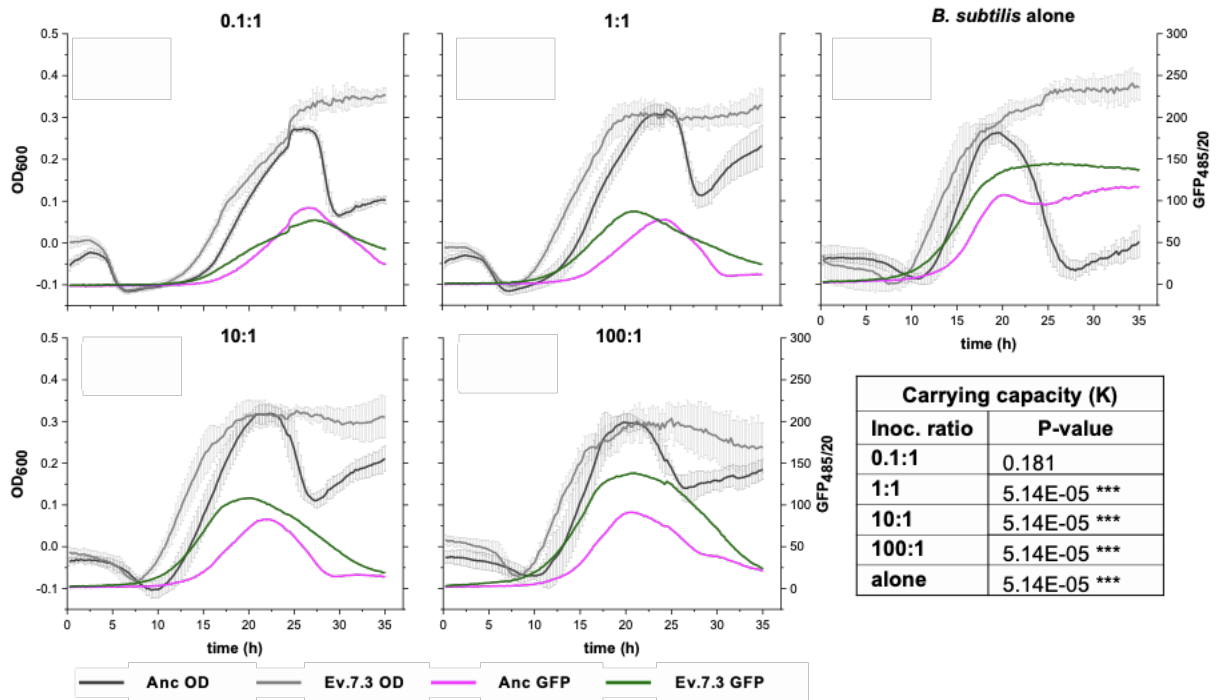


Figure S6: Ev7.3 shows enhanced carrying capacity in MSNc + xylan when co-cultured with a semi-synthetic, soil-derived community compared to the ancestor. Related to Figure 6. Growth of constitutively GFP-expressing *B. subtilis* ancestor or Ev7-3 in co-culture with the community in MSNc + xylan (0.5 %) was measured under four different inoculation ratios: 0.1:1, 1:1, 10:1 and 100:1 of *B. subtilis* and community, respectively. OD₆₀₀ and GFP_{485/20nm} were measured every 15 min for 35 h at 24 °C while shaking. Data represents mean and error bars represent standard deviation (N=6-9, 2-3 independent ON cultures with 3 technical replicates each). The carrying capacity (K) was calculated from the GFP_{485/20nm} data. Significant difference in carrying capacity between the ancestor and Ev7.3 under the same inoculation ratio or alone was tested by a Two-sample *t*-test or Wilcoxon Unpaired Two-sample test (when data failed to meet parametric assumptions). *** indicates P<0.001.

B. subtilis vs

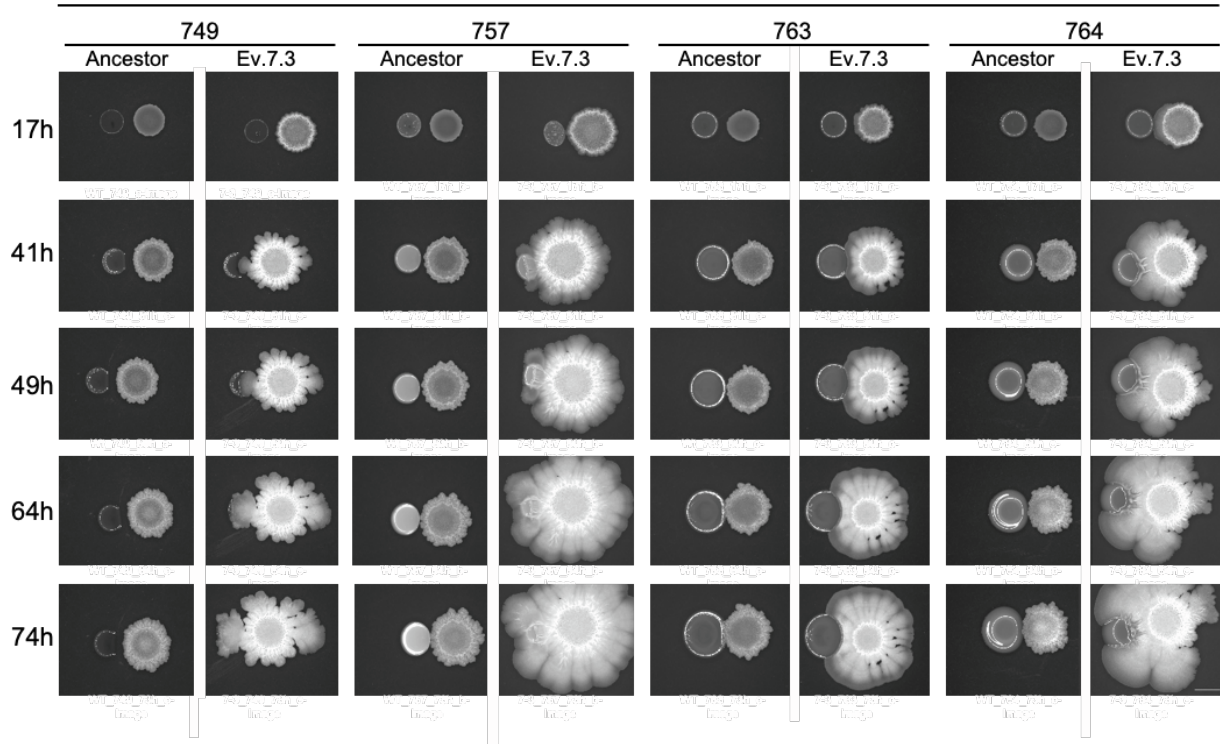


Figure S7: Pairwise interactions of *B. subtilis* ancestor or evolved isolate 7.3 with bacterial species. Related to Figure 6. Ancestor or Ev7.3 was spotted on LB agar (1.5 %) at 0.7 cm distance from bacterial species belonging to *Pedobacter* sp. D749, *Rhodococcus globerulus* D757, *Stenotrophomas indicatrix* D763 or *Chryseobacterium* sp. D764. Plates were incubated at 30 °C and images were captured at the given time points using the stereomicroscope. Ancestor represents *B. subtilis* DK1042. Each colony is a representative of three replicates. Scale bar denotes 5 mm.

Table S1: The table shows detected mutations in the re-sequenced genomes of evolved isolates. Related to Figure 5. The functions of the gene products were retrieved from the SubtiWiki Database (Zhu and Stülke, 2018). T = Transfer.

T12			T18			T30							Position	Gene	Mutation	Function
7.1	7.2	7.3	7.1	7.2	7.3	1.1	6.1	6.2	6.3	7.1	7.2	7.3				
								X					72039	<i>spolIE</i>	Glu489*	protein serine phosphatase,
											X		84980	<i>pabC</i>	Leu24Val	aminodeoxychorismate lyase,
										X		X	235527	Intergenic (<i>glpT/ybeF</i>)	T>C	<i>glpT</i> : glycerol-3-phosphate permease. <i>ybeF</i> : unknown
	X												529455	<i>tRNA</i>	C>T	
		X											578493	<i>ydeS</i>	Ala39Val	unknown regulator (similar to transcriptional regulator (TetR family))
		X											961914	<i>ssuB</i>	483C>T	aliphatic sulfonate ABC transporter
						X							1002530	Intergenic (<i>glpP/glpF</i>)	G>T	<i>glpP</i> : transcriptional antiterminator, regulation of glycerol and glycerol-3-phosphate utilization. <i>glpF</i> : glycerol facilitator, glycerol uptake
							X	X	X				1002601	<i>glpF</i>	Cys22_Val25del	glycerol facilitator, glycerol uptake
		X				X							1073693	<i>scoC</i>	Ala21Asp	transition state regulator
							X						1221482	<i>oppA</i>	Thr534Asn	oligopeptide ABC transporter
							X		X				1471759	<i>kinA</i>	Gly568Val	two-component sensor kinase, initiation of sporulation
												X	1472932	<i>patA</i>	138G>A	aminotransferase, biosynthesis of lysine and peptidoglycan
		X											1528830	<i>pdhA</i>	474G>T	pyruvate dehydrogenase, links glycolysis and TCA cycle
X													1567847	<i>ylbD</i>	p.Glu56*	outer spore coat protein,
						X							1573820	<i>ddcP</i>	*342Leu	DNA damage checkpoint recovery protease
						X							1686014	<i>trmFO</i>	Arg58Ser	tRNA:m(5)U-54 methyltransferase, tRNA modification
							X		X				1702691	<i>fliM</i>	p.Arg326Ile	flagellar motor switch protein, movement and chemotaxis
							X		X				1947405	<i>galU</i>	672C>T	UTP--glucose-1-phosphate uridylyltransferase
										X			2026710	<i>yoaE</i>	p.Val427Leu	formate dehydrogenase

						X							2406541	<i>ypbD</i>	His116Asp	unknown
						X							2414116	<i>rsiX</i>	Lys200fs	anti-SigX, control of SigX activity
			X										2422584	<i>spmB</i>	p.Ala81Ser	spore maturation protein (spore core dehydration)
								X					2434346	<i>ypuB</i>	p.Glu9*	hypothetical (unknown)
X			X	X	X				X	X	X		2552672	Intergenic (<i>sinI/sinR</i>)	C>G	<i>sinI</i> : antagonist of SinR <i>sinR</i> : transcriptional regulator, control of biofilm formation
									X				2759185	<i>sacC</i>	Arg304fs	levanase, degradation of levan to fructose
						X							2893562	<i>leuA</i>	150C>A	2-isopropylmalate synthase, biosynthesis of leucine
			X										3005087	<i>tcyN</i>	Gly19Val	cystine ABC transporter (ATP-binding protein), cystine uptake
											X		3070742	<i>ythQ</i>	Glu226Asp	<i>ythQ</i> = function unknown, similar to ABC transporter
									X		X		3141769	<i>ythB</i>	948G>A	cytochrome bd2, menaquinol oxidase, respiration
									X		X		3409591	<i>sigO</i>	Met139del	RNA polymerase sigma factor
			X	X									3498891	<i>yvfR</i>	Arg127Ile	ABC transporter (ATP-binding protein)
		X											3537728	<i>levB</i>	His70Tyr	endolevanase, levan degradation
				X									3547528	<i>pgmB</i> (<i>pgcM</i> ?)	Asp14Tyr	beta-phosphoglucomutase, starch and maltodextrin utilization
		X											3570846	<i>glmR</i>	Pro223His	regulator of carbon partitioning between central metabolism and peptidoglycan biosynthesis
						X							3666013	<i>gtaB</i>	Cys116Phe	UTP-glucose-1-phosphate uridylyltransferase, biosynthesis of teichoic acid
						X							3666017	<i>gtaB</i>	A>G	
						X							3666019	<i>gtaB</i>	.Arg118Pro	
						X							3666048	<i>gtaB</i>	Val128Leu	
						X							3666050	<i>gtaB</i>	A>T	
						X							3666059	<i>gtaB</i>	T>A	
						X							3666080	<i>gtaB</i>	Glu138Asp	
						X							3672992	<i>yvzE</i>	Leu2Arg	

					X								3673014	<i>yvzE</i>	27T>C	putative UTP-glucose-1-phosphate uridylyltransferase
								X					3679471	<i>tagE</i>	His330Tyr	UDP-glucose:polyglycerol phosphate glucosyltransferase, biosynthesis of teichoic acid
		X	X										3679534	<i>tagE</i>	Glu309*	
					X					X	X	X	3679795	<i>tagE</i>	Glu222*	
						X		X					3679856	<i>tagE</i>	Trp202fs	
					X								4025538	<i>wapA</i>	Asn1683fs	cell wall-associated protein precursor, intercellular competition
					X								4151147	<i>walH</i>	Arg252Thr	negative effector of Walk, controls cell wall metabolism
		X											4152067	<i>walk</i>	Asp554Tyr	two-component sensor kinase, control of cell wall metabolism
						X	X	X					4152909	<i>walk</i>	Thr273Lys	